



# High-resolution fingerprints of past landsliding and spatially explicit, probabilistic assessment of future reactivations: Aiguettes landslide, Southeastern French Alps

Jérôme Lopez Saez <sup>a,b,\*</sup>, Christophe Corona <sup>c</sup>, Markus Stoffel <sup>c,d</sup>, Frédéric Berger <sup>a</sup>

<sup>a</sup> Cemagref UR EMGR, 2 rue de la Papeterie, BP 76, F38402 St-Martin-d'Hères cedex, France

<sup>b</sup> Institut de Géographie Alpine, Laboratoire Politiques publiques, Action Politique, Territoires (PACTE), UMR 5194 du CNRS, Université Joseph Fourier, 14 bis avenue Marie Reynoard, 38100 Grenoble, France

<sup>c</sup> Laboratory of Dendrogeomorphology (dendrolab.ch), Institute of Geological Sciences, University of Berne, Baltzerstrasse 1 + 3, CH-3012 Berne, Switzerland

<sup>d</sup> Climatic Change and Climate Impacts, Institute for Environmental Sciences, University of Geneva, 7 Route de Drize, CH-1227 Carouge, Switzerland

## ARTICLE INFO

### Article history:

Received 16 November 2011

Received in revised form 7 April 2012

Accepted 30 April 2012

Available online 14 May 2012

### Keywords:

Dendrogeomorphology

Landslide

Poisson distribution model

Probability maps

Threshold precipitation

## ABSTRACT

The purpose of this study was to reconstruct spatio-temporal patterns of past landslide reactivation and the possible occurrence of future events in a forested area of the Barcelonnette basin (Southeastern French Alps). Analysis of past events on the Aiguettes landslide was based on growth-ring series from 223 heavily affected Mountain pine (*Pinus uncinata* Mill. ex Mirb.) trees growing on the landslide body. A total of 355 growth disturbances were identified in the samples indicating 14 reactivation phases of the landslide body since AD 1898. Accuracy of the spatio-temporal reconstruction is confirmed by historical records and aerial photographs. Logistic regressions using monthly rainfall data from the HISTALP database indicated that landslide reactivations occurred due to above-average precipitation anomalies in winter. They point to the important role of snow in the triggering of reactivations at the Aiguettes landslide body. In a subsequent step, spatially explicit probabilities of landslide reactivation were computed based on the extensive dendrogeomorphic dataset using a Poisson distribution model for an event to occur in 5, 20, 50, and 100 yr. High-resolution maps indicate highest probabilities of reactivation in the lower part of the landslide body and increase from 0.28 for a 5-yr period to 0.99 for a 100-yr period. In the upper part of the landslide body, probabilities do not exceed 0.57 for a 100-yr period and somehow confirm the more stable character of this segment of the Aiguettes landslide. The approach presented in this paper is considered a valuable tool for land-use planners and emergency cells in charge of forecasting future events and in protecting people and their assets from the negative effects of landslides.

© 2012 Elsevier B.V. All rights reserved.

## 1. Introduction

Landslides are a major driver of landscape changes and evolution by transferring sediment from sources to sinks (Guzzetti et al., 2005). The occurrence of mass movements has recently become a topic of major interest for both researchers and local administrators, especially in relation with the assessment of landslide hazards and risks (Magliulo et al., 2008). The increasing interest in landslides certainly reflects the increasing awareness of the socio-economic significance of landslides (Aleotti and Chowdhury, 1999) but also indicates quite clearly that human pressure on the environment has become more important for land development and urbanization (Petrascheck and Kienholz, 2003). An appropriate assessment of existing and potential future landslide hazards requires, among others, a detailed determination of the spatial and temporal occurrences of landslides at the site level. However, major obstacles normally exist for such studies due to the lack of reliable historical records on the frequency and localization of past events (Aleotti and

Chowdhury, 1999). As a consequence, past research focused more on landslide susceptibility (see Guzzetti, 2000 and references therein for a review) rather than on the documentation of landslide hazards.

By contrast, comparatively few attempts have been undertaken to establish the temporal frequency of slope failures in the past. In previous work historical records were reconstructed for single landslides or landslide-prone regions and estimates were usually derived from existing archives such as narrations, historical documents, terrestrial or aerial photographs, remote sensing series, incidental statements or, more rarely, from public historical databases (e.g., Brunnsden et al., 1976; Coe et al., 2000; Crovelli, 2000; Guzzetti et al., 1994; Hovius et al., 1997; Martin et al., 2002). Yet, the temporal window of such records only seldom spans more than a few decades and almost never covers centuries. In addition and even more importantly, archival data on landslides have normally not been recorded for geomorphic purposes. As a result, they lack spatial completeness, resolution and precision and invariably emphasize events that caused damage to human structures (Mayer et al., 2010). At the same time, they tend to underestimate failures, even large ones, which took place in areas that have been not been populated in the past (Carrara et al., 2003; Guzzetti et al., 1994; Ibsen, 1996). Finally, there are also considerable problems in interpretation because of the

\* Corresponding author at: Cemagref UR EMGR, 2 rue de la Papeterie, BP 76, F38402 St-Martin-d'Hères cedex, France. Tel.: +33 476762833.

E-mail address: [Jerome.lopez@cemagref.fr](mailto:Jerome.lopez@cemagref.fr) (J. Lopez Saez).

changing standards and criteria of reporting in archival records over time (Ibsen, 1996).

In forested shallow landslides, the use of tree rings may greatly help the documentation of past events and may allow reconstruction of

accurate chronologies of landslide reactivations over considerable periods in the past. According to Carrara and O'Neill (2003), the first investigators to use tree rings to date landslides were McGee (1893) in Tennessee and Fuller (1912) in Mississippi. However, modern

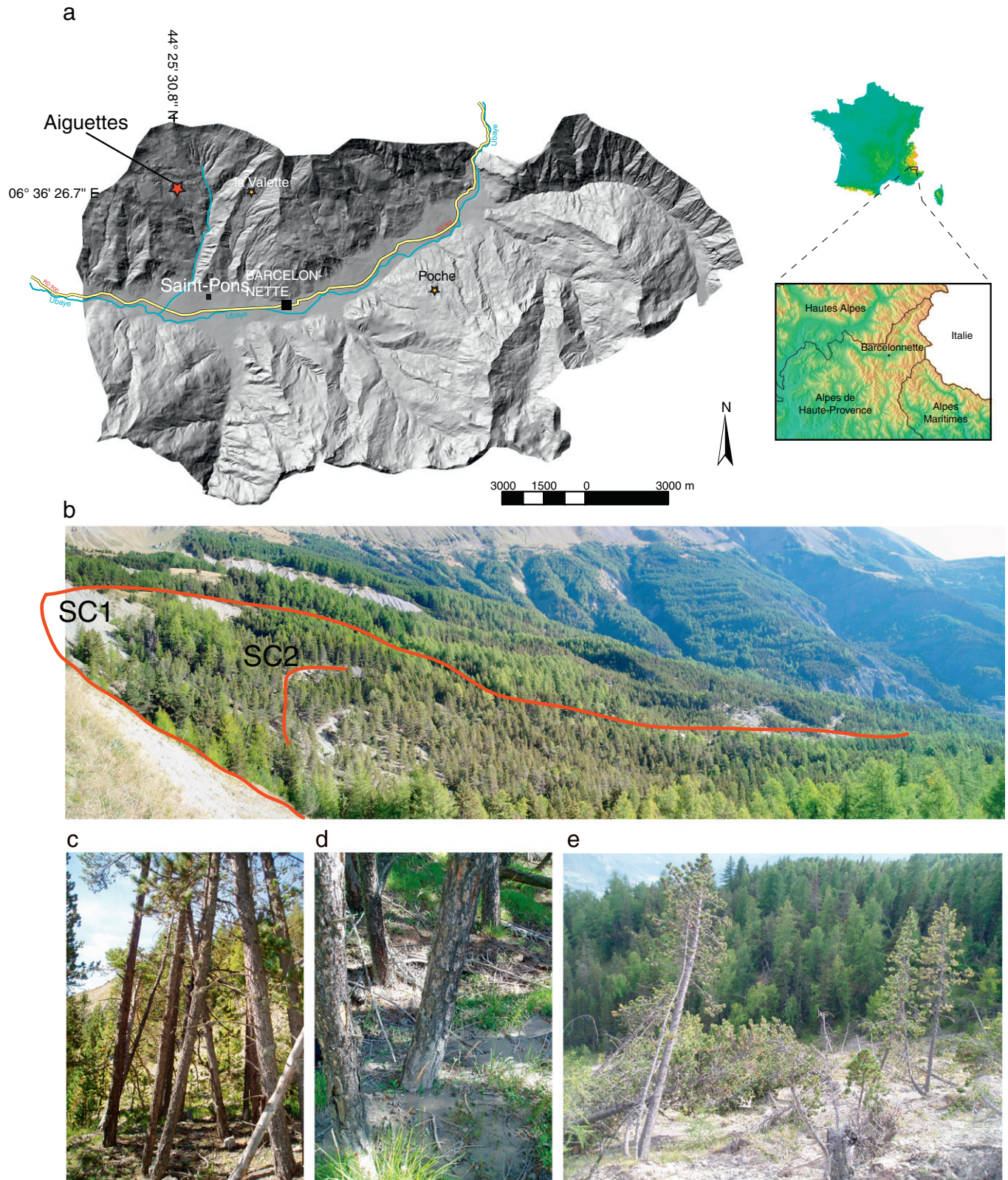


**Fig. 1.** (a) The Aiguettes landslide is located in the Southeastern French Alps, in the Ubaye Valley, near the village of Saint-Pons. (b) View of the two main scarps (SC1 and SC2) and of the landslide body. The red line delimits the scarps. View of (c) tilted trees and (d) buried trunk bases in the landslide body. (e) Trees affected by a recent earthflow (1780 m–1820 masl).

dendrogeomorphology dates back to the early 1970s (Alestalo, 1971) and the information contained in tree-ring records has been used extensively in the United States (e.g., Carrara, 2007; Jensen, 1983; Reeder, 1979; Shroder, 1978 for a recent review) ever since. In Europe, tree rings have been used to document landslide reactivations in the French (e.g. Astrade et al., 1998; Braam et al., 1987; Lopez Saez et al., 2011a, 2011b) and Italian Alps (Fantucci, 1999; Stefanini, 2004), the Spanish Pyrenees (Corominas and Moya, 1999) or the Flemish Ardennes (Van Den Eckhaut et al., 2009). Whereas these studies focused on the overall activity or possible triggers of landslides, they did neither define the temporal frequency of reactivation for specific areas nor address the probability of future events to occur in certain compartments on the landslide body. However, the localization of past and potential future landslide reactivation along with a detailed assessment (i.e. sub-annual resolution) of actual landslide triggers appears key for a better understanding of the process and for the management of sites at risk.

The purpose of this study therefore was to provide a high-resolution, spatio-temporal chronology of reactivations on a forested, shallow (4–9 m) landslide body located in the Ubaye Valley (Alpes de Haute-Provence, France). The specific goals of this study were to (i) derive periods of landslide reactivation with sub-annual resolution using the dendrogeomorphic record of 223 Mountain pine (*Pinus uncinata* Mill. ex Mirb.) trees and to (ii) compare results with historical archives to evaluate the spatio-temporal accuracy of the reconstruction. In addition, (iii) single-point data on past landslides was then compiled to derive a high-resolution landslide return period map for the landslide body and (iv) to quantify and map the probability of landslide reactivation for the coming 5, 20, 50, and 100 yr, using a Poisson distribution. In a final step, (v) the coincidence between

landslide reactivations and extreme precipitation was examined in order to improve existing threshold values for the triggering of major landslides in the French Alps.

## 2. Study site

The Aiguettes landslide (44°25'31"N, 6°36'27"E, Fig. 1a) is located in the Riou-Bourdoux catchment, on the north-facing slope of the Barcelonnette basin, 3 km north of Saint-Pons (Alpes de Haute-Provence, France). The Riou-Bourdoux catchment, a small tributary of the Ubaye River, has been considered the most hazardous torrential area in France and is well known for its extensive mass-movement activity (Delsigne et al., 2006; Lopez Saez et al., 2011b). The Aiguettes landslide body is 800 m long, 400 m wide (16 ha) and ranges from 1740 to 1980 masl (Fig. 2). Geology is characterized by a 9-m thick top layer of morainic colluvium formed of blocks of Triassic limestone and dolomite buried in a sandy matrix. The colluvium is underlain by autochthonous Callovo-Oxfordian black marls (Stien, 2001; Utasse, 2009) which are very sensitive to weathering and erosion (Antoine, 1995). The area is characterized by a dry and mountainous Mediterranean climate with strong inter-annual rainfall variability. According to the HISTALP dataset (Efthymiadis et al., 2006), precipitation at the gridded point closest to the Aiguettes landslide (44°25'N, 6°35'E) is  $895 \pm 154 \text{ mm yr}^{-1}$  for the period 1800–2003. Rainfall can be violent, with intensities trespassing  $50 \text{ mm h}^{-1}$ , especially during frequent summer storms. Melting of the thick snow cover, which forms during the cold months from December to March, only adds to the effect of heavy spring rain (Flageollet, 1999). Mean annual temperature is  $7.5 \text{ }^\circ\text{C}$  with  $130 \text{ d yr}^{-1}$  of freezing (Maquaire, 2003).

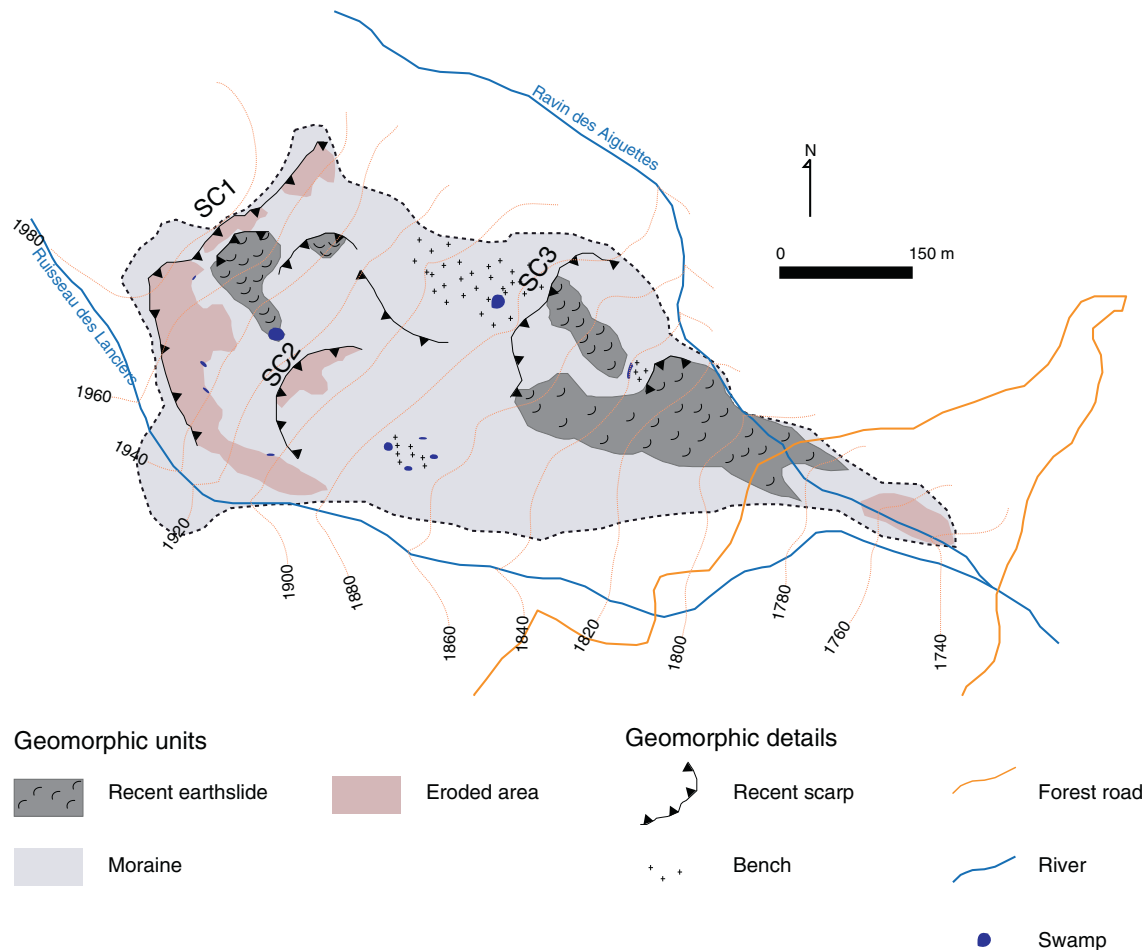
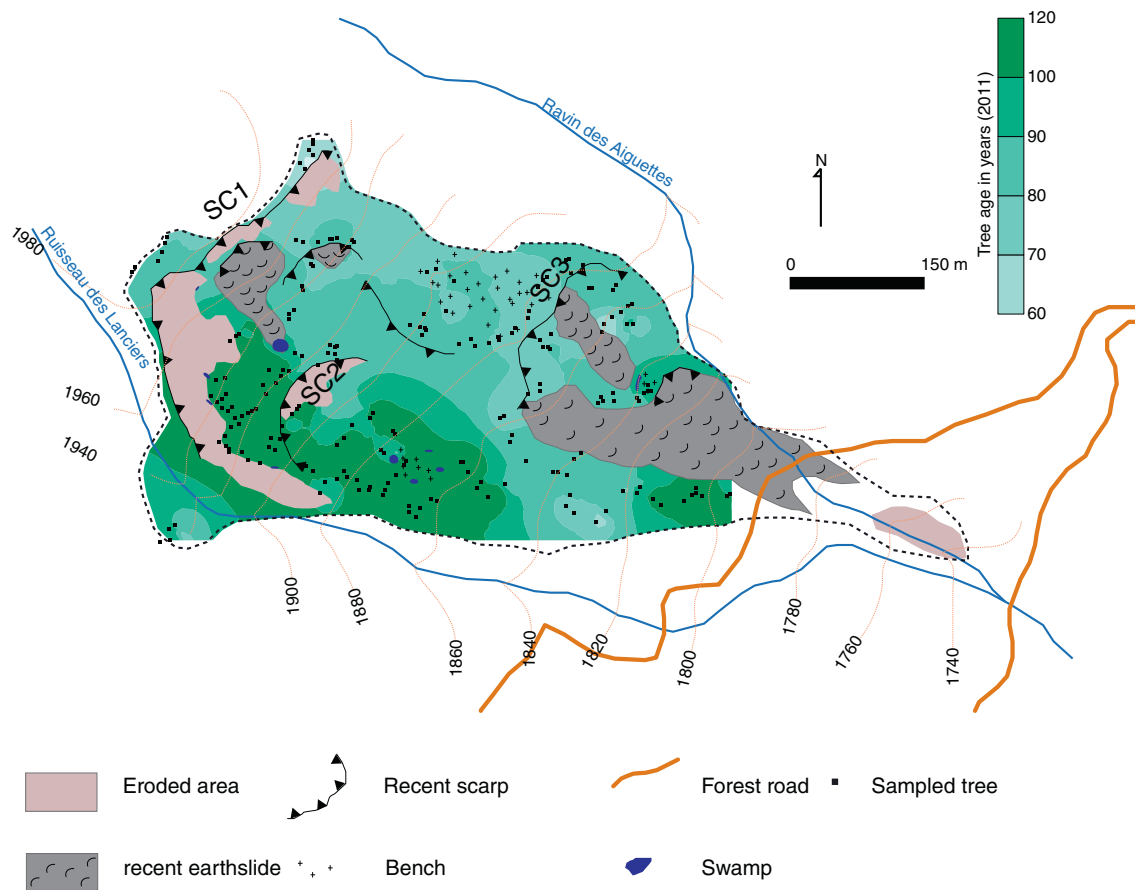


Fig. 2. Geomorphic map of the Aiguettes landslide body (adapted from Utasse, 2009).



**Fig. 3.** Location and mean age of the 212 *P. uncinata* trees sampled at Aiguettes. Interpolation was performed using the Geostatistical Analyst (ESRI, 2005) and an inverse distance weighted interpolation.

These predisposing geomorphic and climatic factors explain the occurrence of a large rotational landslide which usually affects the uppermost 4–9 m of the top moraine layer (Stien, 2001; Utasse, 2009). The study site is characterized by irregular topography with a mean slope angle of  $\sim 20^\circ$ . Three main scarps (SC) delineate the head of the landslide (Figs. 1b and 2): SC1, located at  $\sim 1980$  masl, is 200 m long and 40 m high, with a slope angle of  $30^\circ$ , and completely void of vegetation; SC2, located at  $\sim 1920$  masl, is 25 m high, with a slope angle of  $30^\circ$ , and partly colonized by trees; and SC3, located at  $\sim 1880$  masl, is 40 m high, with a slope angle of  $70^\circ$  and is not vegetated. In this sector, a recent earth slide is clearly visible (Figs. 1e and 2). *P. uncinata* has a competitive advantage on these dry, poor soils (Dehn, 1999) and forms nearly homogeneous forest stands outside the surfaces affected by the scarps and recent earth slides. The tilted and deformed *P. uncinata* trees also clearly indicate that the Aiguettes landslide has been affected by multiple reactivations in the past (Fig. 1c,d,e).

### 3. Material and methods

#### 3.1. Collection and preparation of samples

Based on an outer inspection of the stem, *P. uncinata* trees influenced by past landslide activity were sampled. Four cores per tree were extracted; two in the supposed direction of landslide movement (i.e. up-slope and downslope cores), and two perpendicular to the slope. To gather the greatest amount of data on past events, trees were sampled within the tilted segment of the stems. To avoid misinterpretation, trees growing in sectors influenced by processes other than landslide or anthropogenic activity (sylviculture) were not sampled for analysis. A total of 223 disturbed *P. uncinata* trees were sampled resulting in 892 increment cores.

For each tree, additional data was collected, such as (i) tree height; (ii) diameter at breast height; (iii) visible defects in tree morphology, and particularly the number of knees; (iv) position of the extracted sample on the stem; (v) photographs of the entire tree; and (vi) data on neighboring trees. Tree coordinates were obtained with an accuracy  $< 1$  m with a Trimble GeoExplorer GPS. In addition, 20 undisturbed *P. uncinata* trees located above the landslide scarps and showing no signs of landslide activity or other geomorphic processes were sampled to establish a reference chronology. Two cores per tree were extracted, parallel to the slope direction and systematically at breast height. The reference chronology represents common growth variations in the area (Cook, 1990) and enables precise cross-dating and aging of the cores sampled on the landslide body. The samples obtained in the field were analyzed and data processed following standard dendrochronological procedures (Braker, 2002; Stoffel and Perret, 2006). Single steps of surface analysis included sample mounting on a slotted mount, drying, and surface preparation by finely sanding the upper core surface up to grit size 600. In the laboratory, tree rings were counted and rings measured to the nearest 0.01 mm using a digital LINTAB positioning table connected to a Leica stereomicroscope and TSAP-WIN Scientific software (Rinntech, 2009). The reference chronology was developed based on the growth curves of the undisturbed trees using the ARSTAN software (Cook, 1985). The two measurements of each reference tree were averaged, indexed and detrended using a double detrending procedure (Holmes, 1994) with a negative exponential curve (or linear regression) and a cubic smoothing spline function (Cook, 1990). The quality of the cross-dating was evaluated using COFECHA (Holmes, 1983) as well as the graphical functions of TSAPWin (Rinntech, 2009). Growth curves of the samples of disturbed trees were then compared with the reference chronology to detect missing, wedging or false rings and to identify reactions to mechanical stress. As no

significant correlation was found between the reference chronology and 44 cores from 11 affected trees, we rejected these samples for further analysis.

### 3.2. Age structure of the stand

The age structure of the stand was approximated by counting the number of tree rings of selected trees ( $n = 212$ , 95% of the sampled population) and visualized after an inverse distance weighted interpolation using ArcGIS 9.3 (ESRI, 2005). Interpolations were performed using an ellipse-shaped search including data from ten to fifteen neighboring weighted points. The same method was used for the return period and probability maps. However, since trees were not sampled at their stem base and the piths or innermost rings of several trees were rotten, the age structure might be biased; the map thus only reflects age at sampling height, but neither inception nor germination dates. Nonetheless, it provides valuable insights into major disturbance events at the study site with reasonable precision.

### 3.3. Sign of disturbance in the tree-ring record

Landslide movement induces several kinds of growth disturbances (GD) to trees, most commonly in the form of an abrupt reduction in annual ring width and/or the formation of compression wood (CW) on the tilted side of the stem. A reduction in annual ring width over several years is interpreted as damage to the root system, loss of a major limb, or a partial burying of the trunk resulting from landslide activity (Carrara and O'Neill, 2003). In this study, growth-ring series had to exhibit (i) a marked growth reduction (GR) in annual ring width for at least five consecutive years such that the (ii) width of the first narrow ring was 50% or less of the width of the annual ring of the previous year. The onset of CW is interpreted as a response to stem tilting induced by landslide pressure. Tilted trees try to recover straight geotropic growth (Mattheck, 1993) through the development of asymmetric growth rings, i.e. the formation of wider annual rings with smaller, reddish-yellow colored cells with thicker cell walls (so-called CW; Timell, 1986) on the tilted side and narrow (or even discontinuous) annual rings on the opposite side (Carrara and O'Neill, 2003; Panshin and De Zeeuw, 1970).

In the laboratory, wood anatomical analysis and microscopic observation focused on CW formation. Based on data from neighboring sites (Rolland and Florence-Schueller, 1998), we know that the vegetation period of *P. uncinata* locally starts at the end of May with the formation of thin-walled early earlywood (EE) tracheids. The transition from late earlywood (LE) to latewood (L) occurs in mid-July and the formation of thick-walled tracheids ends in early October. The period between October and May is called the dormancy (D), and there is no cytogenesis

during this time of the year (Stoffel et al., 2005). The intra-annual position of CW was used in this study to determine the moment of tilting (for more details and illustrations on the seasonality of CW formation see Lopez Saez et al. (2011a) and references therein).

### 3.4. Dating of events

Determination of events was based on the number of samples showing GD in the same year and on the spatial distribution of affected trees on the landslide body (Bollschweiler et al., 2008). To avoid overestimation of GD within the tree-ring series in more recent years because of the larger sample of trees available for analysis, we used an index value ( $I_t$ ) as defined by Butler and Malanson (1985):

$$I_t = \left( \frac{\sum_{i=1}^n (R_t)}{\sum_{i=1}^n (A_t)} \right) \cdot 100. \tag{1}$$

Where  $R$  is the number of trees showing a GD as a response to a landslide event in year  $t$ , and  $A$  is the total number of sampled trees alive in year  $t$ . Following disturbance by an initial event, a tree may not necessarily yield useful data on additional events for some time (i.e. a tree may already be forming a narrow band of annual rings such that a subsequent disturbance would not be detected; Stoffel et al., 2010); this is why  $I_t$  was adjusted to only take account of trees with a useful record for year  $t$  (Carrara and O'Neill, 2003). A minimum of 10 trees exhibiting a response was required for a major reactivation to be dated so as to avoid an overestimation of relative response numbers resulting from a low number of trees early in the record (e.g. Corona et al., 2010, 2012; Dubé et al., 2004).

In order to minimize the risk that GD caused by other (geomorphic) processes could mistakenly be attributed to a landslide event and to take account of the sample size, the chronology of past events was also based on  $I_t > 5\%$ . However, the strictness of these thresholds and the large sample size may induce a misclassification of minor reactivation. To avoid misclassification, the annual patterns of disturbed trees for years with  $5\% > I_t > 2\%$  and GD in  $\geq 5$  trees were carefully examined. Using GPS coordinates, trees were placed into a Geographical Information System (GIS; ESRI, 2005) as geo-objects, and GD were linked as attributes to each single tree. We computed autocorrelations based on the location and GD values of trees with the ArcGIS pattern analysis module and calculated yearly Moran indices (Moran, 1950) to evaluate whether the pattern of disturbed trees was clustered, dispersed or random. A Moran index value near 1 indicates clustering while a value near  $-1$  indicates dispersion. The Z scores and  $p$ -values were used to indicate the significance of individual Moran index values. Random and dispersed patterns

**Table 1**

Growth disturbances corresponding to past landslide reactivations listed by year and type. GD = growth disturbance, GR = growth reduction, CW = compression wood, EE = early earlywood, LE = late earlywood, L = latewood.

Year (n)	Year	GD (n)	GR (n)	CW (n)	EE (%)	LE (%)	L (%)
2004	2004	18	17	1	100	0	0
1998	1998	42	41	1	100	0	0
1996	1996	36	28	8	62	0	38
1982	1982	10	5	5	100	0	0
1979	1979	27	11	16	75	25	0
1977	1977	19	11	8	87	13	0
1971	1971	12	8	4	75	0	25
1961	1961	40	33	7	72	14	14
1936	1936	29	7	22	82	9	9
1934	1934	10	1	9	77	0	23
1916	1916	24	18	6	100	0	0
1912	1912	8	1	7	85	15	0
1904	1904	10	0	10	100	0	0
1898	1898	10	2	8	75	25	0
total	Total	295	183	112	85	7.5	7.5

were disregarded from the reconstruction whereas years with clustered patterns were considered as minor or spatially limited movements.

### 3.5. Calculation of landslide return periods and probabilities of reactivation

Traditionally, the return period designates the mean time interval at which a material reaches a given point in an avalanche path (Corona et al., 2010; McClung and Schaerer, 1993), with frequency being usually expressed in years as a “return period” (i.e. 1/frequency). We adapted this approach and, by analogy, calculated individual tree return periods ( $R_p$ ) for the Aiguettes landslide from GD frequency  $f$  for each tree  $T$  following the approach presented by Reardon et al. (2008):

$$f_T = \left( \sum_{i=T}^n \text{GD} \right) \div \left( \sum_{i=T}^n A \right) \quad (2)$$

where GD represents the number of growth disturbances detected in tree  $T$ , and  $A$  the total number of years tree  $T$  was alive.

The exhaustive sampling of trees, the dendrogeomorphic reconstruction and the unusually complete landslide record covering a comparably long time span was then used to perform a probabilistic landslide analysis. The theoretical probability for a landslide to occur at Aiguettes was modeled using a Poisson distribution (Corominas and Moya, 2010; Crovelli, 2000; Guzzetti, 2000; Lopez Saez et al., 2011b). The Poisson model allows determination of future landslide probability based on the assumptions (Guzzetti et al., 2005)

that (i) the number of landslide events that occurs at disjoint time intervals is independent; (ii) the probability of an event occurring in a very short time is proportional to the time interval; (iii) the probability of more than one event in a short time interval is negligible; (iv) the probability distribution of the number of events is the same for all time intervals of fixed length; and that (v) the mean recurrence of future events will remain the same as it was observed in the past. In reality, however, most hazardous events, including landslides, are probably not independent and do not occur randomly (Coe et al., 2000). For example, the reactivation of a landslide may make the landslide body more or less susceptible to future activity, thus creating stability or instability in the future. Also, changing land use, local changing climatic conditions or implementation of landslide mitigation measure may consequently make the occurrence of landslides more or less likely in the future (Chleborad et al., 2006). Nevertheless, the Poisson model possibly represents the most appropriate approach for studies where no information other than the mean rate of event occurrence is available. Under such circumstances, the Poisson model provides a good first-cut estimate for the probability of event occurrence in the future (Coe et al., 2000). Based on the above considerations, the probability  $p$  for an event with a return period  $T$  to occur in a given number of years  $N$  (fixed to 5, 10, 20 and 100 years) was computed as follows:

$$p = 1 - e^{-(N/T)}. \quad (3)$$

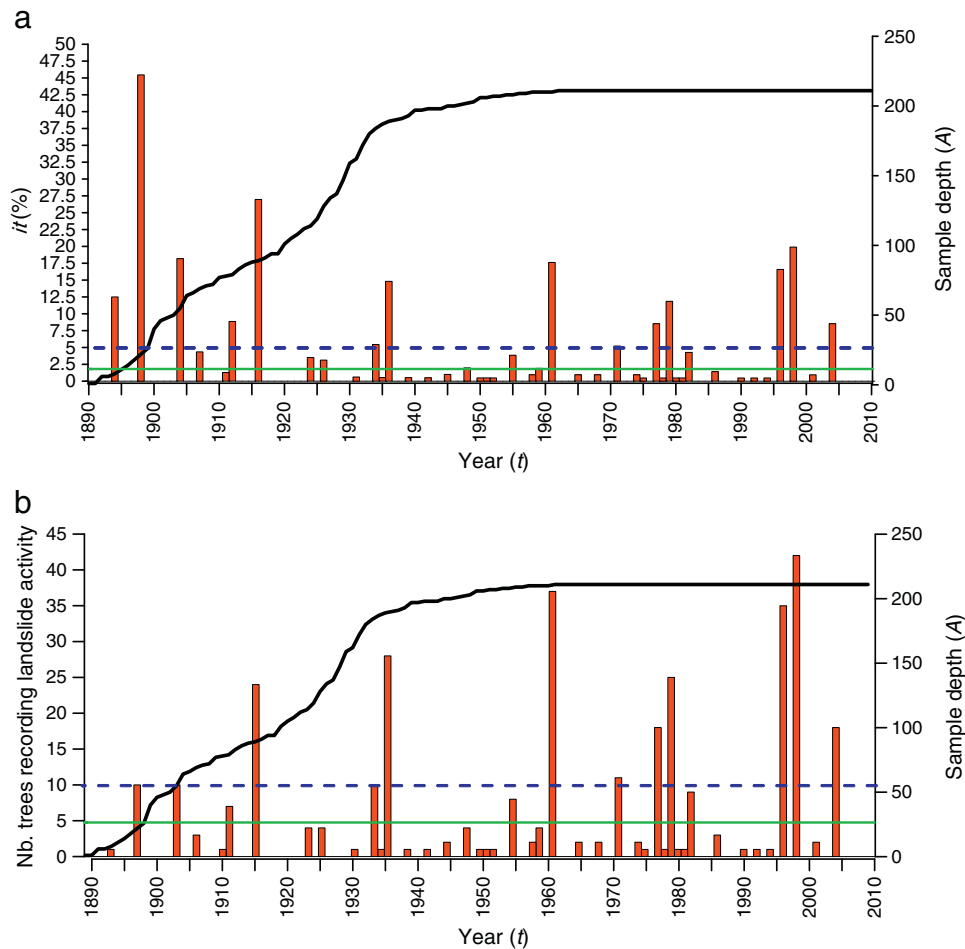


**Fig. 4.** Event response histograms showing landslide induced growth disturbances (GD) from sampled trees: (a) Percentage of trees and (b) total number of trees responding to a damaging event. The blue (green) horizontal dotted line demarcates the 5% (2%) sample depth thresholds in (a), and the  $n = 10$  ( $n = 5$ ) tree thresholds in (b). The black line shows the sample depth (i.e. the total number of trees alive in each year). A total of 14 landslide reactivations could be reconstructed from the tree-ring series since AD 1898.

According to this distribution, the probability for a centennial event to occur during the next 100 years is, for example,  $p = 0.63$ .

### 3.6. Analysis of meteorological conditions leading to landslide reactivation

The relationship between the actual triggering of landslides and rainfall depends on the characteristics of the movement: shallow landslides are commonly triggered by heavy rains falling in the hours or days preceding an event, whereas deeper landslides are usually related to the total rainfall recorded over several weeks or months, and deep-seated movements can even be related to the yearly amounts of precipitation (e.g., Corominas and Moya, 1999; Flageollet, 1999; Stefanini, 2004).

Dendrogeomorphology may yield dates of landslide reactivation with sub-annual or up to seasonal accuracy (Lopez Saez et al., 2011a), but the exact timing of landslide reactivation within a dendrochronological year will remain unknown (Corominas and Moya, 1999). For these reasons, this study did not focus on the relationship between landslide occurrences and heavy rainfall over short periods, but rather considered mean monthly values to provide an appropriate level of resolution for analyses. Monthly homogenized precipitation records were

taken from the HISTALP dataset (Efthymiadis et al., 2006) consisting of a dense network of 192 meteorological stations extending back to AD 1800 and covering the Greater Alpine Region (4–19°E, 43–49°N, 0–3500 masl). It consists of station data gridded at  $0.1^\circ \times 0.1^\circ$  latitude and longitude, which were  $44^\circ 25' N$  and  $6^\circ 35' E$  for this study. The correlation coefficients (not presented) between the HISTALP series and the observed records from the Barcelonnette meteorological station (available for the period 1954–2003) are significant at  $p < 0.05$  for all months. Several classification and regression tree (CART; Breiman et al., 1984; Ripley, 1996) analyses have been used in the past to predict landslide reactivation years from the set of historic climate data (Hebertson, 2003) using the rpart routine (Therneau and Atkinson, 1997) of the R package (R Development Core Team, 2007). CART is a statistical method which explains the variation of a response variable (i.e. landslide index  $I_L$  in the present case) using a set of explanatory independent variables, so-called predictors (i.e. monthly climatic data). The method is based on a recursive binary splitting of the data into mutually exclusive subgroups within which objects have similar values for the response variable (see Breiman et al., 1984 for details). Several CART models were tested for our study with monthly, seasonal and annual combinations

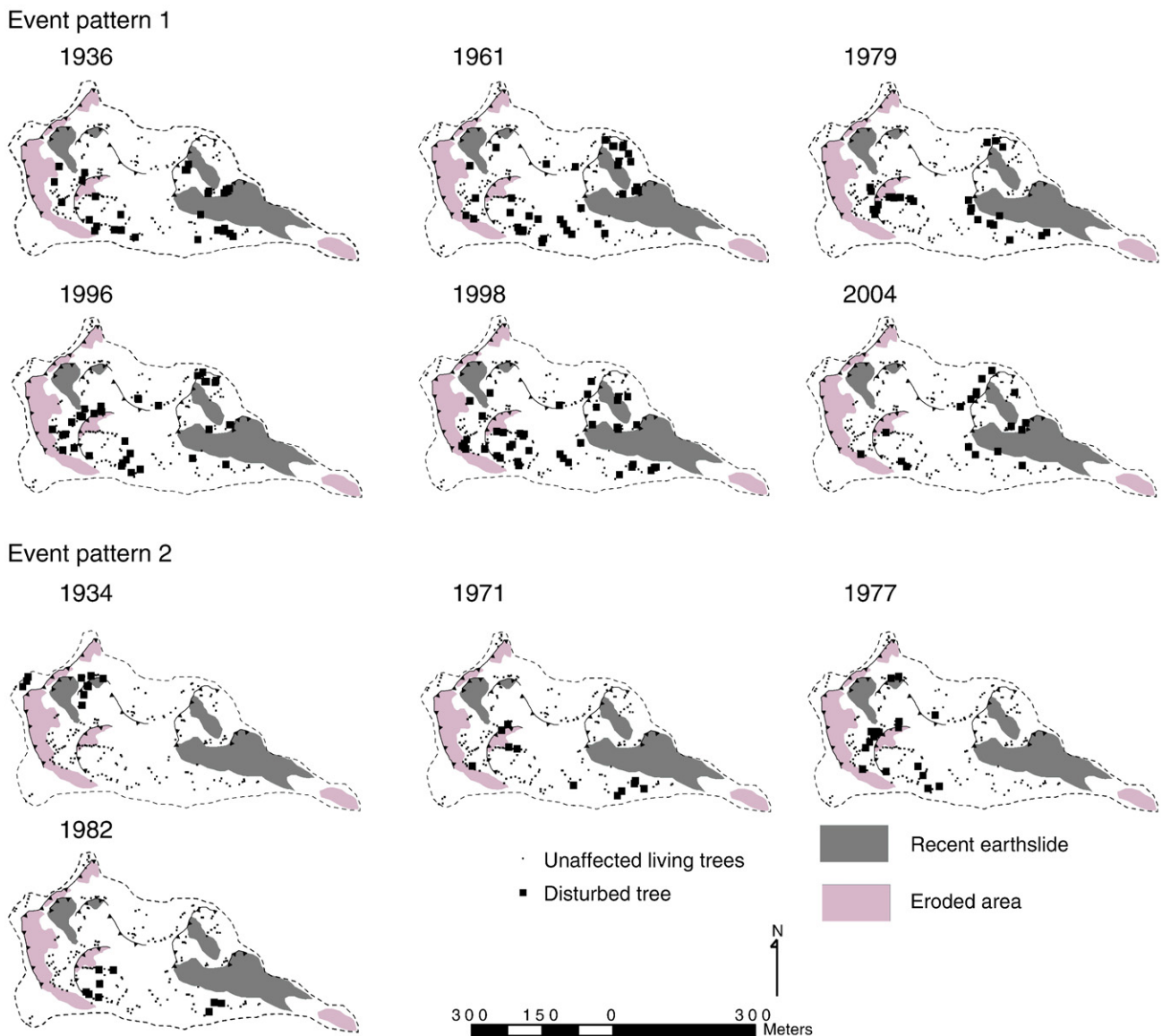


Fig. 5. Event-response maps showing the Aiguettes landslide for each of the reconstructed reactivation events. Large squares indicate trees affected by the mass movement, small squares represent trees which were alive but did not show any signs of disturbance in that particular year.

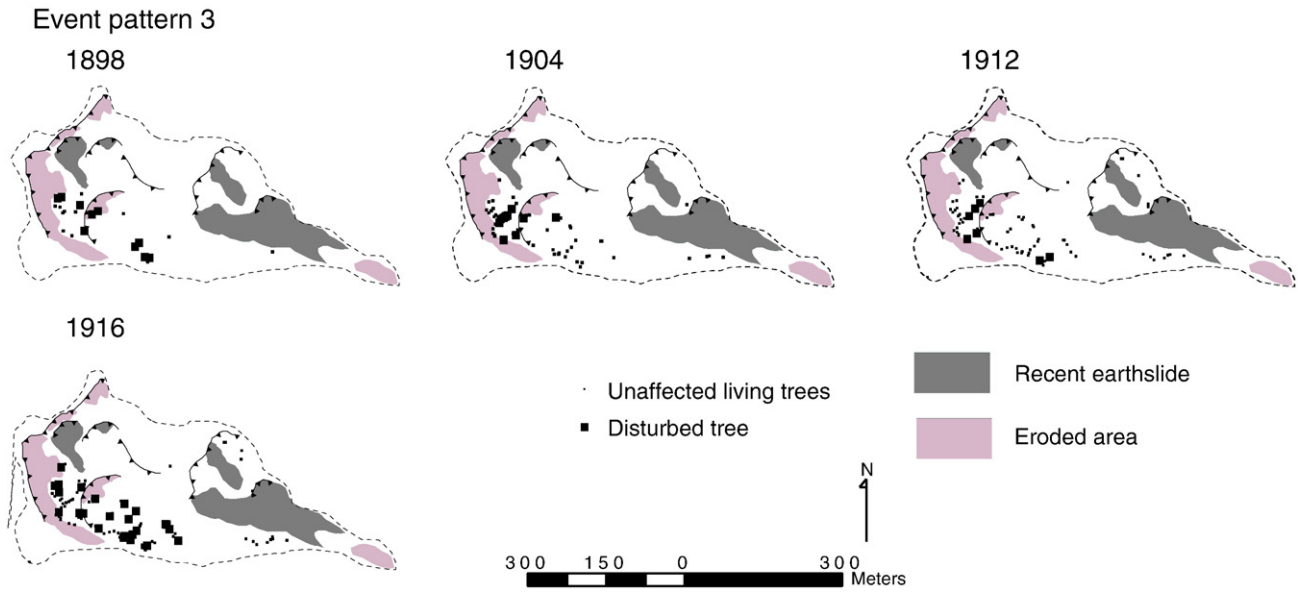


Fig. 5 (continued)

of predictors and years from 1898 to 2003 and grouped into two response classes. Years with  $I_t < 5\%$  were attributed to class 0, and years with  $I_t > 5\%$  and clustered patterns were defined class 1. Predictors were chosen to cover a large time range so as to evaluate a potential delay between rainfall, landslide triggering and GD formation (Timell, 1986). Monthly precipitation totals from previous June to current September were successively tested as predictors. The relation between climatic variables and landslide reactivation was further explored using logistic regression (Aldrich and Nelson, 1984; Hebertson, 2003; Lopez Saez et al., 2011a). This method describes the relationship between a

dichotomous response variable, the presence/absence of a landslide reactivation in our case, and a set of climatic data. It addresses the same questions as a least squares regression (OLS). In the logistic regression, however, one estimates the probability that the outcome variable assumes a certain value rather than estimating the value itself by fitting data to a logistic curve. The logit is simply the log odds ratio of mean landslide reactivation probability:

$$\text{logit}(p_i) = \frac{p_i}{(1-p_i)} \tag{4}$$

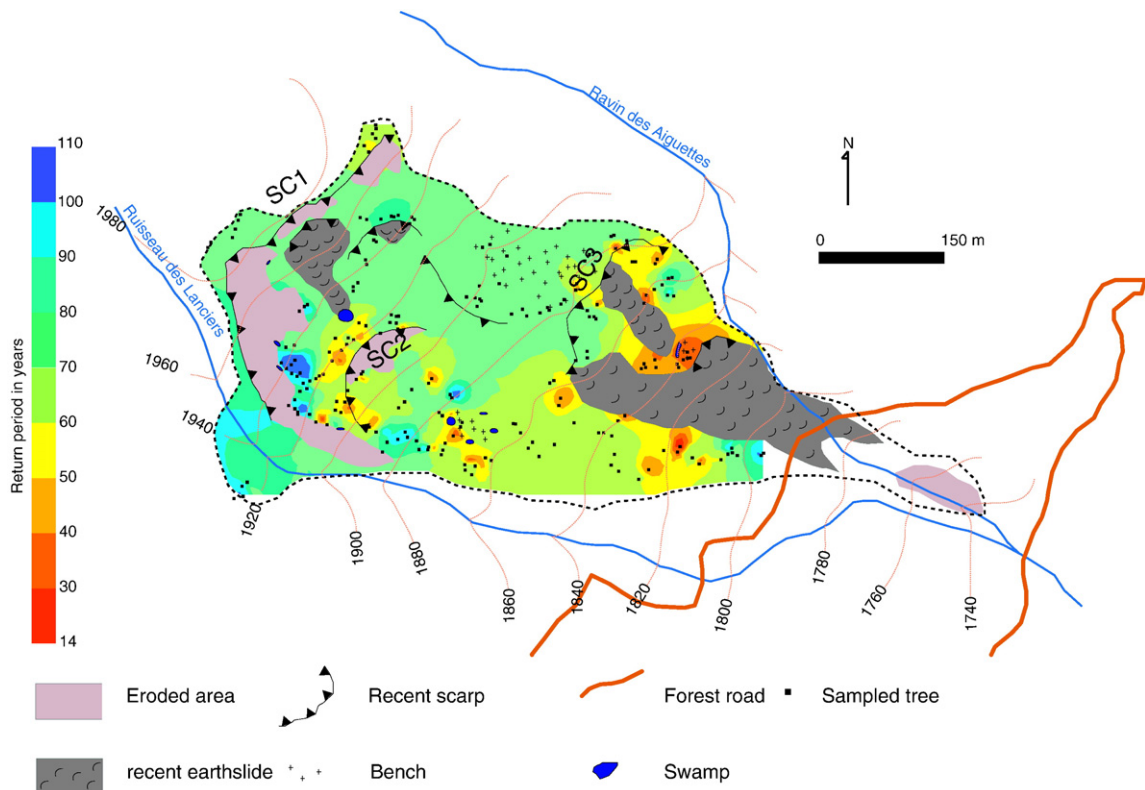


Fig. 6. Interpolated return periods for the sampled area of the Aiguettes landslide. The calculation of return period maps was based on the entire tree-ring sample and for the period 1890–2010.

where  $p$  is the probability of a major landslide reactivation year for  $i$  years (1898–2003 herein). It is modeled as a linear function:

$$\text{logit}(p_i) = \beta_0 + \beta_1 \chi_{1,i} + \dots + \beta_k \chi_{k,i} \tag{5}$$

with an equivalent formulation:

$$p_i = \frac{1}{1 + e^{-(\beta_0 + \beta_1 \chi_{1,i} + \dots + \beta_k \chi_{k,i})}} \tag{6}$$

where  $\chi_k$  represents the  $k$  climatic factors used as regressors for year  $i$ ,  $\beta_0$  the intercept, and  $\beta_k$  the regression coefficients. The unknown parameter  $\beta_j$  is usually estimated by maximum likelihood using a method common to all generalized linear models.

#### 4. Results

##### 4.1. Age structure of the stand and growth disturbances

After cross-dating, data on the pith age from 212 *P. uncinata* trees growing on the Aiguettes landslide suggest an average age of the sample of  $91 \pm 16$  yr. The oldest tree selected for analysis shows 120 rings at sampling height (AD 1890), while 60 growth rings (AD 1950) were counted in the youngest tree. As can be seen from Fig. 3, the distribution of tree ages is characterized by two dominant age classes said 60–90 and 90–120 yr. When an age correction factor is added to take account of the sampling height, inception dates for seedlings can be attributed to two phases in the 1880s and 1910s. Our data also show that trees aged 60–90 yr constitute the forest matrix. Older trees (>90 yr) are restricted to (i) a large patch in the southern part of the landslide body (1850–1950 masl); and to (ii) a smaller patch located in the lower part of the landslide body, at the southern margin of a recent earth slide (1780–1820 masl).

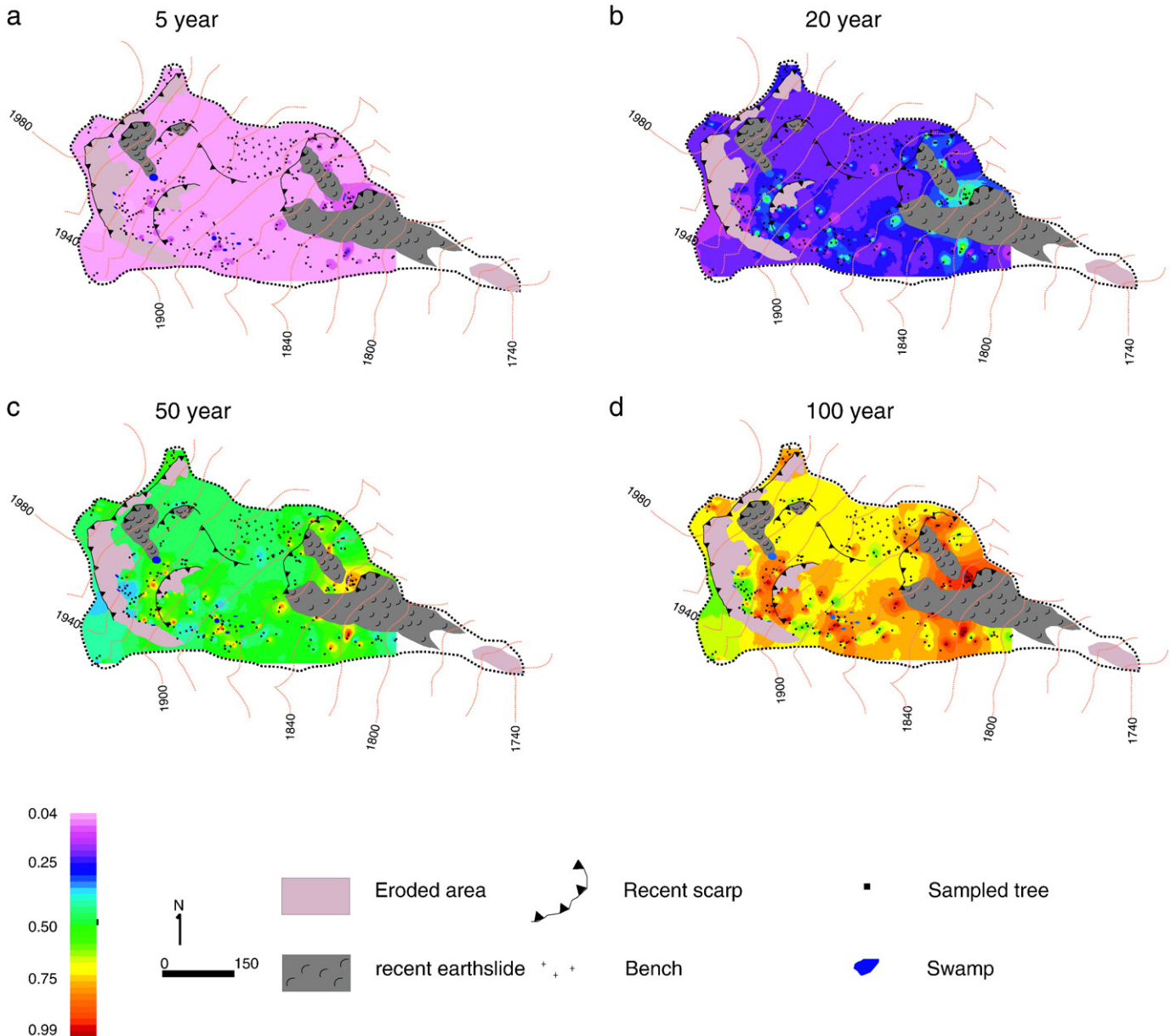


Fig. 7. Probability maps of reactivation for the Aiguettes landslide within the next (a) 5, (b) 20, (c) 50, and (d) 100 yr obtained with a Poisson distribution model.

A total of 355 GD relating to past landslide reactivations were identified in the 212 disturbed trees for the period 1898–2010. The most common reaction to landslide reactivations was the presence of abrupt GR with 60% of all GD (213 GD). The onset of compression wood (142 GD, 40%) represents another common response of disturbed *P. uncinata* trees to landsliding. Trees with CW were used to determine the intra-seasonal timing of tilting at Aiguettes. As can be seen from Table 1, CW formation clearly concentrates to EE (92%). Considering the timing of annual tree-ring formation at Aiguettes, we conclude that tilting preferentially occurred between October of the previous and April of the year showing CW.

In AD 1892, sample depth surpassed the  $n = 5$  trees threshold for GD to be considered minor landslide reactivation events. Sample depth increased markedly after AD 1900 and surpassed 50% ( $n = 106$ ) of the total population in 1922. The earliest GD was recorded in 1894, however, a landslide reactivation was not inferred for this year as GD were restricted to one tree (Fig. 4a,b).

#### 4.2. Landslide reactivations

In total, 15 years did exceed the 2% threshold for  $I_t$  (Fig. 4a) with  $\geq 5$  trees exhibiting a GD (Fig. 4b) between 1898 and 2004. Twelve major reactivations with  $GD > 10$  and  $I_t > 5\%$  were reconstructed in 1898, 1904, 1911, 1916, 1936, 1961, 1971, 1977, 1979, 1996, 1998, and 2004 (Fig. 4a,b). For the years 1912, 1955, and 1982, the number of GD was  $> 5$  and  $5\% > I_t > 2\%$ ; these years could not be considered reactivation events with equal confidence and were therefore further tested with yearly Moran  $I$  statistics. Results point to a spatial clustering with sufficient aggregation in 1912 (0.18) and 1982 (0.14); these were considered years with landslide reactivation. In 1955, Moran  $I$  statistics point to a dispersed distribution of affected trees ( $-0.01$ ) with no significant pattern; this year was not therefore kept for further analysis.

#### 4.3. Spatial distribution of trees disturbed by landslide reactivations

The spatial distribution of disturbed trees by the same landslide reactivation is of considerable help for the determination of the spatial extent of past reactivation. Event-response maps are provided in Fig. 5 and yielded three general patterns for landslide reactivation at Aiguettes. In 1936, 1961, 1979, 1996, 1998, and 2004, landslide reactivation affected trees being affected by scarps SC2 and SC3 (event pattern 1). Event pattern 2 is represented with the landslide reactivations of 1934, 1971, 1977 and 1982. In this case, GD are restricted to isolated segments of the landslide body. For instance, the reactivation of 1934 only disturbed trees located in the northern segment of the landslide body below SC1. Event pattern 3 is illustrated with the reactivations of 1898, 1904, 1912 and 1916. GD are restricted to the upper part of the landslide body, near SC2. However, the real spatial extent of these reactivations could not be determined, as only the oldest trees growing on the landslide body could be used for analysis for these early-20th century events.

#### 4.4. Return period and landslide probability maps

Considering the 14 reactivations within the sampled area, the mean return period for the Aiguettes landslide is  $0.11 \text{ event yr}^{-1}$  for the period 1891–2010. The number of reactivations clearly increases from 3 yr for the period 1921–1970 to 7 yr for the period 1971–2010. Maximum decadal frequencies (3 events) are observed in 1971–1980. Conversely, no event was reconstructed in the 1921–1930 and 1941–1960. Within the area sampled, return periods range from 14 to 70 years below 1880 masl (Fig. 6). Minimal return periods ( $< 30$  yr) are reconstructed downslope from SC2. Conversely,

the least affected compartment of the landslide body is restricted to its south-westernmost part.

In a subsequent step, return periods of landslide reactivation were transformed into landslide occurrence probability using a Poisson distribution. High-resolution maps of return period derived from the 212 cross-dated disturbed trees were used to represent the probability for a landslide reactivation to occur within 5, 20, 50, and 100 yr (Fig. 7a–d). As expected, the probability for a landslide to be reactivated is highest near SC2 and increases from 0.28 for the 5-yr to 0.99 for the 100-yr period. At the margins, probabilities for a new landslide event are lower; yet, they remain  $> 0.57$  for the 100-yr period.

#### 4.5. Relationship between landslide occurrences and meteorological data

At Aiguettes, the best model derived from CART analyses used winter precipitation to optimize splitting event probabilities. Splitting values for winter total precipitation was 398 mm, and the confusion matrix indicates that the model classified correctly non-landslide years in 94% of the cases. The likelihood of correctly classifying landslide reactivation is 60%. Several logistic regression models were tested with the presence (absence) of landslide reactivation as a dichotomous response variable and with monthly, seasonal, and annual rainfall as a single predictor. Analyses confirmed the primordial role of winter total precipitation (from December to April, hereafter referred to as DJFMA) in landslide triggering (Table 2) and the most parsimonious logistic regression model after backward elimination has the general form:

$$\text{logit}(p_i) = \beta_0 + \beta_j(\text{DJFMA rainfall}).$$

The model provides parameter estimates of  $-7.62$  for  $\beta_0$  and  $0.015$  for  $\beta_j$ .  $\beta_j$  indicates that the probability of a landslide reactivation was estimated to increase by 0.017 with a respective 1 mm increase in mean DJFMA rainfall. The likelihood ratio test, significant at  $p > 0.001$  indicates that the logit model is better than a null model and is correctly predicting landslide triggering probability. The probability of a landslide is 15% for 393 mm winter rainfalls (i.e. ninth decile threshold for winter precipitation; see Fig. 8) and 50% for 505 mm of rainfall.

**Table 2**

Parameters used for the logistic regression models of triggering: for each month, the  $p$  value, its significance, the intercepts (A) and slopes (B) are given. Blank cells are not statistically significant,  $p < 0.1$ ,  $*p < 0.05$ ,  $**p < 0.01$ ,  $***p < 0.001$ .

Month	$p$ value	Significance	A	B
Jun (n – 1)	0.277		0.006	–2.92
Jul (n – 1)	0.502		0.005	–2.68
Aug (n – 1)	0.802		–0.001	–2.17
Sep (n – 1)	0.742		0.001	–2.47
Oct (n – 1)	0.493		0.002	–2.59
Nov (n – 1)	0.612		0.002	–2.54
Dec (n – 1)	0.0004	***	0.024	–4.03
Jan	0.0206	*	0.018	–3.28
Feb	0.085	.	0.012	–3.01
Mar	0.122		0.012	–3.08
Apr	0.212		0.007	–2.94
May	0.475		–0.005	–1.84
Jun	0.967		–0.0002	–2.28
Jul	0.694		0.003	–2.53
Aug	0.678		–0.003	–2.094
Sep	0.0683		–0.014	–1.32
Dec (n – 1) + Jan + Feb + Mar + Apr (n)	0.0003	***	0.015	–7.62

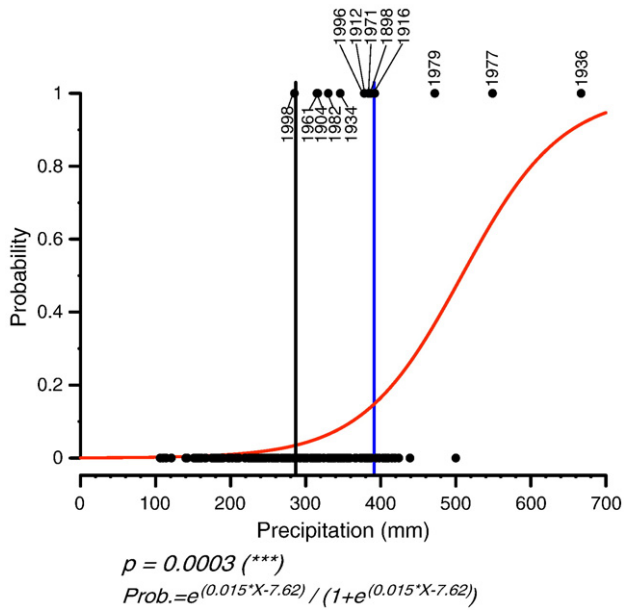


**Fig. 8.** Winter precipitation (December to April) values and predicted probabilities of triggering for the Aiguettes landslide. Monthly values for the period 1890–2003 are extracted from the HISTALP database.

**5. Discussion**

*5.1. Spatio-temporal accuracy of the reconstruction*

Dendrogeomorphic analysis of 848 increment cores and four cross-sections taken from 212 Mountain pine (*P. uncinata*) trees allowed reconstruction of 14 reactivations phases of the Aiguettes landslide between 1890 and 2010. The reconstructed time series represents a minimum frequency of reactivation events for the Aiguettes landslide in the recent past as the reconstruction was limited by tree age. A photograph from 1890 (Fig. 9) does not show a continuous forest in the Aiguettes area and therefore supports our data suggesting tree germination and the establishment of a forest at the study site around the end of the 19th century. In addition, the forested patch located between SC1 and SC2 present in Fig. 9 confirms the older ages obtained with tree-ring analysis (Fig. 3). Furthermore, the existence of SC1 and SC2 on the photograph reveals that the first occurrence of landslides at Aiguettes predates the oldest dendrogeomorphic event dated to 1898.

Several limitations became apparent as to the potential of tree-ring analysis in detecting landslide events. First of all, only reactivations powerful enough to damage trees (e.g., topping, tilting, or

root disrupture) will remain visible in the dendrogeomorphic record. The more violent and destructive events are, however, capable of killing trees and evidence of this category of events is not likely to be available to the investigator, as dead trees will disappear some time after an event. Second, our reconstruction was limited by the age of the trees established on the landslide body, an element which is partly linked to the frequency of destructive events. Third, it is also obvious that a tree recovering from an initial landslide event and forming very narrow annual rings or CW will not necessarily develop a signal after a subsequent reactivation that is different enough for it to be clearly distinguishable from the first event (Carrara and O’Neill, 2003).

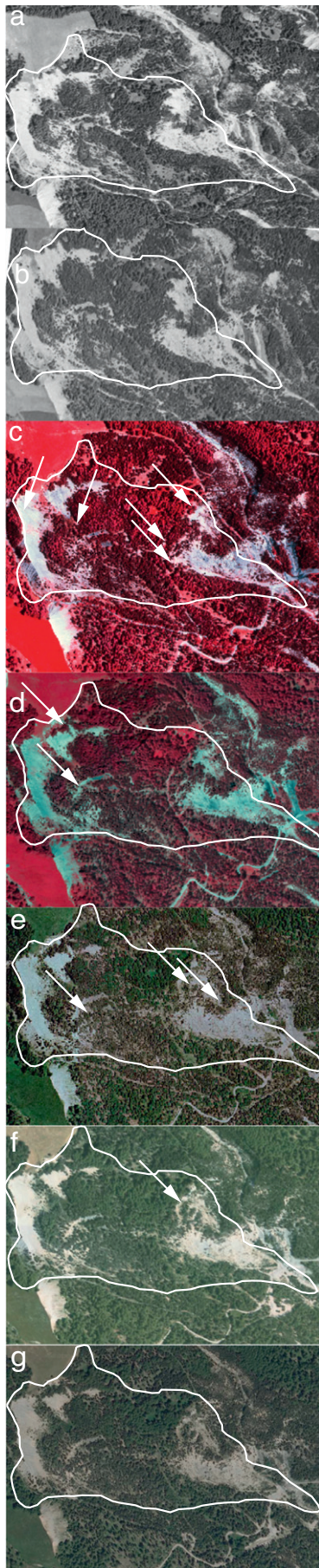
Despite these limitations, the methodology deployed in this study clearly has the potential to reconstruct past landslide events at the local level. In addition, the  $I_t$  and GD thresholds as well as the spatial analysis of event-response maps minimized the risk of GD resulting from non-landslide events to be included in the chronology. The thresholds also allowed rejection of GD related to creep or fall which have been shown to affect a rather limited number of trees per event (Stoffel and Perret, 2006).

For the period 1948–2007, the diachronic analysis of aerial photographs provides additional evidence for the spatio-temporal accuracy of the dendrogeomorphic reconstruction presented in this paper. Between 1948 and 1956 (Fig. 10a), the diachronic analysis does not reveal significant movement at Aiguettes. This observation agrees with the absence of reactivations observed in the dendrogeomorphic record. The reactivations of 1961 and 1971, deciphered from the tree-ring records, are supported by the slight extension of bare areas observed in the central part of scarps SC1 and SC3 between 1956 (Fig. 10b) and 1974 (Fig. 10c). Between 1974 and 1982 (Fig. 10d), the diachronic analysis suggests significant changes with a longitudinal extension of SC1 and SC2. These changes thus support the assumption of three reactivations reconstructed in 1977, 1979, and 1982 for which event-response maps clearly indicate disturbed trees around SC2. Between 1982 and 2004 (Fig. 10e,f), bare areas appear preferentially downslope of SC3 and secondarily around SC2. These evolutions corroborate the event-response maps reconstructed for the events in 1996, 1998, and 2004. Finally, between 2004 and 2010 (Fig. 10g), no reactivation is observed neither on the aerial photographs nor in the dendrogeomorphic reconstruction.

Fig. 11 shows a comparison of our reconstructed landslide reactivations (Fig. 11a) with historical archives of (i) debris flows in the Riou Bourdoux catchment (1890–1994, Fig. 11b), where Aiguettes is located, and of (ii) landslide events in the wider Barcelonnette region (1890–2003, Fig. 11c). The historical archive of debris flows in the Riou Bourdoux catchment (Delsigne et al., 2006) contains 41 events in 28 distinct years between 1890 and 1994 and suffers from a major gap during the interwar period (1918–1947). Only four



**Fig. 9.** View of the Aiguettes landslide from the west facing slope of the Riou Bourdoux catchment in AD 1890. (Data from the archives of the Restauration des Terrains en Montagne (RTM), used with permission).



years coincides between the two records, namely 1898, 1977, 1979, and 1982 (Fig. 11a,b). Conversely, five landslide events are not synchronous with debris-flow activity in the Riou Bourdoux catchment and 35 debris flows do not have any analogues with reconstructed landslides.

Additionally, the dendrogeomorphic time series of landslides from Aiguettes was compared with a continuous record of archival data on 138 landslides and mudslides in the Barcelonnette area (Amiot and Nexon, 1995; Flageollet, 1999). For sites located in the vicinity of the Aiguettes landslide, isolated events have been noted for 1904 and 1911, landslide activity at four locations in 1936 and 1977, at five sites in 1982 and 1996, and even on nine different landslide bodies in 1971 (Fig. 11a,c). When compared with the reconstructed Aiguettes series, eight years coincides between the two series, but analogues cannot be found for six dates, namely 1898, 1912, 1934, 1961, 1979, and 1998 and therefore remain unconfirmed. If the comparison is done at the decadal scale, a scarcity of events can be observed at the local (Aiguettes) and regional scales between 1912 and 1933. For the period 1980–1990, the Aiguettes reconstruction shows a complete absence of landslides whereas an increase in landslide frequency is observed at the regional scale, partly related to the triggering of mudslides at La Valette and Super Sauze (Malet, 2003).

## 5.2. Rainfall conditions for landslide reactivation

Analysis of the meteorological datasets spanning more than 110 yr (1890–2003) indicated that December and more largely winter (from December to April) precipitation were significantly related to the probability of reactivation of the Aiguettes landslide. The highest probabilities of reactivations systematically corresponded with above average winter precipitation (> 285 mm), while low precipitation resulted in relatively low probabilities. Additionally, three out of four years with precipitations > 450 mm corresponded with landslide reactivations, namely in 1936, 1977, and 1979.

These results are consistent with (i) the wood anatomical analysis, where the onset of CW in EE for reactivation years (Table 1) corresponds to events which occurred during dormancy of trees (i.e. between October and April; Lopez Saez et al., 2011a), but (ii) may also explain the poor synchronicity observed between the Riou Bourdoux record of debris flows and our landslide reconstruction. Although precipitations certainly play a crucial role in the triggering of both processes, intense summer rainfalls capable to generate debris flows in the Riou Bourdoux catchment (Remaître, 2006) are not probably strong enough to cause reactivations of the Aiguettes landslide.

As typical for shallow landslides (Schuster and Wiczorek, 2002), we hypothesize that the combined effect of snowmelt and high DJFMA precipitation totals would be the main trigger of landslide activity at Aiguettes. Analysis of the mean altitude of the Aiguettes landslide and mean nivometric coefficients in the Ubaye Valley (ranging between 20% and 86% at 1700 masl in April; Boisvert, 1955) underlines the importance of snow in landslide reactivations at Aiguettes and in the entire Barcelonnette basin (Flageollet, 1999). For example, the landslide of May 26, 1971 was triggered after a winter rich in snow and a very wet spring (265.5 mm between March 14 and May 26, measured at Barcelonnette; Flageollet, 1999). Similarly, the landslide at La Valette near Barcelonnette that occurred in March 1982 is acknowledged by a number of authors (e.g., Evin, 1990) to have been triggered as a consequence of heavy spring rain falling on a melting snow cover.

**Fig. 10.** Diachronic evolution of the Aiguettes landslide between 1948 and 2009. Aerial photographs of the landslide in (a) 1948 (National Geographic Institute, aerial mission, 1948\_F, 363537\_3540\_P\_30000), (b) 1956 (1956\_F, 3139–3639\_P\_25000), (c) 1974 (1974\_FR\_2620\_P\_11000), (d) 1982 (1982\_IFN04\_P\_17000), (e) 2000 (2000\_FD04\_C\_25000), (f) 2004 (2004\_FD04\_C\_80), and (g) 2009 (2009\_FD04\_C\_30). The white line delineates the Aiguettes landslide body, white arrows indicate areas with landslide movements.

More generally, the European Alps have had repeated instances of snowmelt-triggered landslides, such as the Hohberg landslide (1030–1790 masl) in the Swiss Prealps where a sudden acceleration was observed following heavy snowfall, a warming period and heavy rainfall (Schuster and Wieczorek, 2002), or (ii) the Falli Hölli landslide (Swiss Prealps; 1560–1645 masl) which moved about 200 m in 1994 due to three periods of snowmelt (Raetzo-Brülhart, 1997). At the European scale, 4233 landslides were triggered in Central Italy by a sudden change in temperature on 1 January 1997, resulting in extensive melting of the snow cover (e.g., Guzzetti et al., 2002). Similarly, at the end of March 2006, the Czech Republic witnessed a fast thawing of an unusually thick snow cover in conjunction with massive rainfall and more than 90 shallow landslides in the Moravian region (Bil and Müller, 2008).

5.3. Probability maps for landslide reactivation

The reconstruction of spatio-temporal patterns of landslide activity with dendrogeomorphic techniques is relatively recent but has proven helpful for the understanding of landslide kinematics and its spatial evolution (Corominas and Moya, 2010). In our study, the exhaustive sampling of disturbed *P. uncinata* trees allowed reconstruction of a very detailed spatio-temporal chronology of landslide reactivation at Aiguettes. Given the completeness of the reconstruction extending back to AD 1898, we were able to map return periods of landslide reactivation. Assuming that landslide recurrence will

remain comparable in the future, and adopting a Poisson probability model (Guzzetti et al., 2005), we were also able to determine the probability of having a reactivation in each mapping unit for time intervals varying from 5 to 100 yr. Highest return periods associated with major probabilities of reactivation are mapped in the lower part of the landslide body (SC3 and secondary SC2) on each side of a recent earth slide for SC3. Lower probabilities of reactivation are concentrated in the northern upper part of the landslide body.

Our approach is a field-based reconstruction and willingly does not include statistical analyses or physically-based modeling. It is not the scope of this study to comment on these conventional methods, which have been shown to predict the spatio-temporal occurrence of landslides with difficulties (Jaiswal et al., 2011). Usually, to perform quantitative hazard assessments, the key issue is to translate landslide susceptibility values in terms of spatial probability (Corominas and Moya, 2008). By contrast, the approach presented in this paper, despite the limitations of the Poisson model, allows determination of quantitative probabilities of reactivation estimated directly from the frequency of past landslide events.

6. Conclusion

As human activities increase in mountain areas, landslides have become a more serious social and economic issue. As a consequence improved and more detailed landslide forecasting becomes a prerequisite, even at the local scale. Although nice local studies based on

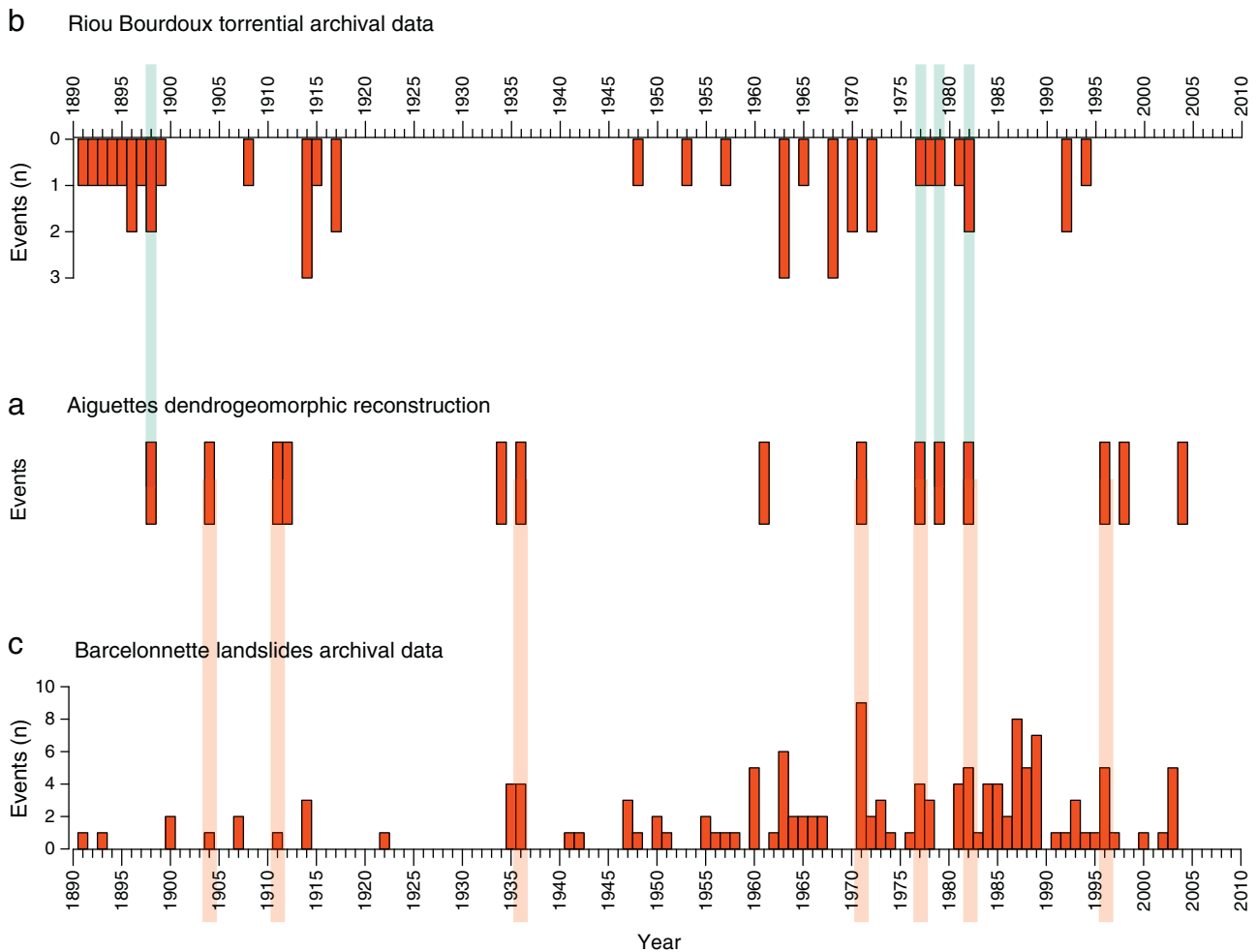


Fig. 11. Comparison of (a) the dendrogeomorphic reconstruction with (b) the Riou-Bourdoux torrential archival data and (c) the regional archives of landsliding in the Barcelonnette basin for the period 1890–2010. Gray (brown) shaded bars indicate coincidence between the reconstruction and the Riou Bourdoux (regional) archives.

physically based modeling of landslides exist for the wider Barcelonnette basin, such assessments are currently difficult to be obtained elsewhere. In this study, we demonstrate the potential of extensive tree-ring analyses for landslide forecasting and show (i) how dendrogeomorphology can add substantially to the spatio-temporal record of landslides at a study site. Many reactivations, which remained unnoticed in archival data, could be identified and mapped and thus help extend the history of landslides back to the late 19th century. Comparison of tree-ring data with historical records and aerial photographs clearly demonstrates the spatio-temporal accuracy of the reconstruction. The approaches used in this paper also helped (ii) to improve our knowledge of the causes of landslide reactivation with respect to meteorological parameters, which is of interest to all those in charge of anticipating landsliding on multi-annual to multi-decadal timescales and to those who are responsible for (iii) the identification and classification of endangered areas. If coupled with a Poisson model, dendrogeomorphic mapping can also improve our knowledge about the probability of reactivation. These probability maps should be used for disaster prevention and generation of risk maps, as well as for the detailed design phase of engineering works and for the construction of slope stabilization works.

## Acknowledgments

This research has been supported by the DENDROGLISS program, funded by the MAIF Foundation and the Cemagref by the PARAMOUNT program, 'Improved Accessibility, Reliability and security of Alpine transport infrastructure related to MOUNTAINOUS hazards in a changing climate', funded by the Alpine Space Programme, European Territorial Cooperation, 2007–2013. It has also been supported by the EU-FP7 project ACQWA (project no. GOCE-20290). The authors are most grateful to two journal reviewers whose insightful comments helped them to improve an earlier version of the paper.

## References

- Aldrich, J., Nelson, F., 1984. Linear probability, logit and profit models. Quantitative Application in the Social Sciences. Sage Publications, Beverly Hills, CA.
- Aleotti, P., Chowdhury, R., 1999. Landslide hazard assessment: summary review and new perspectives. *Bulletin of Engineering Geology and the Environment* 58, 21–44.
- Alestalo, J., 1971. Dendrochronological interpretation of geomorphic processes. *Fennia* 105, 1–140.
- Amiot, A., Nexon, C., 1995. Inventaire des aléas dans le Bassin de Barcelonnette depuis 1850. Mémoire de Maîtrise de Géographie Physique. Université Louis Pasteur, Strasbourg.
- Antoine, P., 1995. Geological and geotechnical properties of the "Terres Noires" in southeastern France: weathering, erosion, solid transport and instability. *Engineering Geology* 40, 223–234.
- Astrade, L., Bravard, J., Landon, N., 1998. Mouvements de masse et dynamique d'un géosystème alpestre: étude dendrogeomorphologique de deux sites de la vallée de Boulc (Diois, France). *Géographie Physique et Quaternaire* 52, 153–166.
- Bil, M., Müller, I., 2008. The origin of shallow landslides in Moravia (Czech Republic) in the spring of 2006. *Geomorphology* 99, 246–253.
- Boisvert, J., 1955. La neige dans les Alpes françaises. Ph.D. thesis. Université de Grenoble. Grenoble, France.
- Bollschweiler, M., Stoffel, M., Schneuwly, D., 2008. Dynamics in debris-flow activity on a forested cone – a case study using different dendroecological approaches. *Catena* 72, 67–78.
- Braam, R., Weiss, E., Burroughs, P., 1987. Spatial and temporal analysis of mass movement using dendrochronology. *Catena* 14, 573–584.
- Braker, O., 2002. Measuring and data processing in tree-ring research – a methodological introduction. *Dendrochronologia* 20, 203–216.
- Breiman, L., Friedman, J., Olshen, R., Stone, C., 1984. Classification and Regression Trees. Chapman & Hall, New-York.
- Brunsdon, D., Jones, D.K.C., Arber, M.A., 1976. The evolution of landslide slopes in Dorset. *Philosophical Transactions of the Royal Society of London. Series A: Mathematical and Physical Sciences* 283, 605–631.
- Butler, D.R., Malanson, G.P., 1985. A history of high-magnitude snow avalanches, southern Glacier National Park, Montana, U.S.A. *Mountain Research and Development* 5, 175–182.
- Carrara, P., 2007. Movement of a large landslide block dated by tree-ring analysis, Tower Falls Area, Yellowstone National Park, Wyoming. Integrated geoscience studies in the greater Yellowstone area—volcanic, tectonic, and hydrothermal processes in the Yellowstone geocosystem: Morgan, L.A., U.S. Geological Survey Professional Paper, pp. 43–49.
- Carrara, P., O'Neill, J., 2003. Tree-ring dated landslide movements and their relationship to seismic events in southwestern Montana, USA. *Quaternary Research* 59, 25–35.
- Carrara, A., Crosta, G., Frattini, P., 2003. Geomorphological and historical data in assessing landslide hazard. *Earth Surface Processes and Landforms* 28, 1125–1142.
- Chleborad, A.F., Baum, R.L., Godt, J.W., 2006. Rainfall thresholds for forecasting landslides in the Seattle, Washington, area—exceedance and probability. USGS Open-File Report 2006-1064.
- Coe, J., Michael, J., Crovelli, R., Savage, W., 2000. Preliminary map showing landslide densities, mean recurrence intervals, and exceedance probabilities as determined from historic records, Seattle, Washington. USGS Open-File Report 00-0303.
- Cook, E., 1985. A time series analysis approach to tree-ring standardization. Ph.D. thesis. University of Arizona, Tucson.
- Cook, E., 1990. Methods of Dendrochronology: Applications in The Environmental Science. Kluwer Academic Publishers; International Institute for Applied Systems Analysis, Dordrecht Netherlands.
- Corominas, J., Moya, J., 1999. Reconstructing recent landslide activity in relation to rainfall in the Llobregat River basin, Eastern Pyrenees, Spain. *Geomorphology* 30, 79–93.
- Corominas, J., Moya, J., 2008. A review of assessing landslide frequency for hazard zoning purposes. *Engineering Geology* 102, 193–213.
- Corominas, J., Moya, J., 2010. Contribution of dendrochronology to the determination of magnitude–frequency relationships for landslides. *Geomorphology* 124, 137–149.
- Corona, C., Rovéra, G., Lopez Saez, J., Stoffel, M., Perfettini, P., 2010. Spatio-temporal reconstruction of snow avalanche activity using tree rings: Pierres Jean Jeanne avalanche talus, Massif de l'Oisans, France. *Catena* 83, 107–118.
- Corona, C., Lopez Saez, J., Stoffel, M., Bonnefoy, M., Richard, D., Astrade, L., Berger, F., 2012. How much of the real avalanche activity can be captured with tree rings? An evaluation of classic dendrogeomorphic approaches and comparison with historical archives. *Cold Regions Science and Technology*. <http://dx.doi.org/10.1016/j.coldregions.2012.01.003>.
- Crovelli, R.A., 2000. Probability models for estimation of number and costs of landslides. USGS Open-File Report 00-249. USGS, Denver, CO.
- Dehn, M., 1999. Modelling future landslide activity based on general circulation models. *Geomorphology* 30, 175–187.
- Delsigne, F., Lahousse, P., Flez, C., Guiter, G., 2006. Le Riou Bourdoux: un "monstre" alpin sous haute surveillance. *Revue Forestière Française* 527.
- Dubé, S., Filion, L., Héty, B., 2004. Tree-ring reconstruction of high-magnitude snow avalanches in the Northern Gaspé Peninsula, Québec, Canada. *Arctic, Antarctic, and Alpine Research* 36, 555–564.
- Efthymiadis, D., Jones, P.D., Briffa, K.R., Auer, I., Böhm, R., Schöner, W., Frei, C., Schmidli, J., 2006. Construction of a 10-min-gridded precipitation data set for the Greater Alpine Region for 1800–2003. *Journal of Geophysical Research* 111. <http://dx.doi.org/10.1029/2005JD006120>.
- ESRI, 2005. ArcGIS 9.2. Redlands, California.
- Evin, M., 1990. Les risques naturels dans un espace montagnard: la haute-Ubaye. *Revue de Géographie Alpine* 123, 175–192.
- Fantucci, R., 1999. Dendrogeomorphological analysis of a slope near Lago, Calabria (Italy). *Geomorphology* 30, 165–174.
- Flageollet, J., 1999. Landslides and climatic conditions in the Barcelonnette and Vars basins (Southern French Alps, France). *Geomorphology* 30, 65–78.
- Fuller, M., 1912. The New Madrid Earthquake, 2nd edition. Center for Earthquake Studies Southeast Missouri State University, Cape Girardeau Mo.
- Guzzetti, F., 2000. Landslide fatalities and the evaluation of landslide risk in Italy. *Engineering Geology* 58, 89–107.
- Guzzetti, F., Cardinali, M., Reichenbach, P., 1994. The AVI project: a bibliographical and archive inventory of landslides and floods in Italy. *Environmental Management* 18, 623–633.
- Guzzetti, F., Malamud, B.D., Turcotte, D.L., Reichenbach, P., 2002. Power-law correlations of landslide areas in central Italy. *Earth and Planetary Science Letters* 195, 169–183.
- Guzzetti, F., Reichenbach, P., Cardinali, M., Galli, M., Ardizzone, F., 2005. Probabilistic landslide hazard assessment at the basin scale. *Geomorphology* 72, 272–299.
- Hebertson, E., 2003. Historic climate factors associated with major avalanche years on the Wasatch Plateau, Utah. *Cold Regions Science and Technology* 37, 315–332.
- Holmes, R., 1983. Computer-assisted quality control in tree-ring dating and measurement. *Tree-Ring Bulletin* 44, 69–75.
- Holmes, R., 1994. Dendrochronology Program Library –Users Manual. Laboratory of Tree-Ring Research, Tucson, Arizona, U.S.A.
- Hovius, N., Stark, C.P., Allen, P.A., 1997. Sediment flux from a mountain belt derived by landslide mapping. *Geology* 25, 231.
- Ibsen, M., 1996. The nature, use and problems of historical archives for the temporal occurrence of landslides, with specific reference to the south coast of Britain, Ventnor, Isle of Wight. *Geomorphology* 15, 241–258.
- Jaiswal, P., van Westen, C.J., Jetten, V., 2011. Quantitative assessment of landslide hazard along transportation lines using historical records. *Landslides*. <http://dx.doi.org/10.1007/s10346-011-0252-1>.
- Jensen, J., 1983. The Upper Gros Ventre landslide of Wyoming: a dendrochronology of landslide events and possible mechanics of failure. *Geological Society of America, Abstract program* 15, 387.
- Lopez Saez, J., Corona, C., Stoffel, M., Astrade, L., Berger, F., Malet, J., 2011a. Dendrogeomorphic reconstruction of past landslide reactivation with seasonal precision: the Bois Noir landslide, southeast French Alps. *Landslides*. <http://dx.doi.org/10.1007/s10346-011-0284-6>.
- Lopez Saez, J., Corona, C., Stoffel, M., Schoeneich, P., Berger, F., 2011b. Probability maps of landslide reactivation derived from tree-ring records: Pra Bellon landslide, southern French Alps. *Geomorphology*. <http://dx.doi.org/10.1016/j.geomorph.2011.08.034>.
- Magliulo, P., Di Lisio, A., Russo, F., Zelano, A., 2008. Geomorphology and landslide susceptibility assessment using GIS and bivariate statistics: a case study in southern Italy. *Natural Hazards* 47, 411–435.

- Malet, J., 2003. Glissements de type écoulement dans les marnes noires des Alpes du Sud. Morphologie, fonctionnement et modélisation hydro-mécanique. Ph.D. thesis. Université Louis Pasteur, Strasbourg.
- Maquaire, O., 2003. Instability conditions of marly hillslopes: towards landsliding or gully? the case of the Barcelonnette Basin, South East France. *Engineering Geology* 70, 109–130.
- Martin, Y., Rood, K., Schwab, J.W., Church, M., 2002. Sediment transfer by shallow landsliding in the Queen Charlotte Islands, British Columbia. *Canadian Journal of Earth Sciences* 39, 189–205.
- Mattheck, C., 1993. Design in der Natur. Reihe Ökologie 1: Rombach Wissenschaft.
- Mayer, B., Stoffel, M., Bollschweiler, M., Hübl, J., Rudolf-Miklau, F., 2010. Frequency and spread of debris floods on fans: a dendrogeomorphic case-study from a dolomite catchment in the Austrian Alps. *Geomorphology* 118, 199–206.
- McClung, D., Schaerer, P., 1993. *The Avalanche Handbook*. Mountaineers, Seattle.
- McGee, W., 1893. A fossil earthquake. *Geological Society of America Bulletin* 411–414.
- Moran, P.A.P., 1950. Notes on continuous stochastic phenomena. *Biometrika* 37, 17–23.
- Panshin, A., De Zeeuw, C., 1970. 3rd edition. *Textbook of Wood Technology*, volume 1. McGraw-Hill, New York, USA.
- Petrascheck, A., Kienholz, H., 2003. Hazard assessment and mapping of mountain risks in Switzerland. In: Rickenmann, D., Chen, C.L. (Eds.), *Debris-flow Hazards Mitigation: Mechanics, Prediction and Assessment*, Rickenmann. Millpress, Rotterdam, Netherlands, Davos, Switzerland, pp. 25–38.
- R Development Core Team, 2007. R: A Language and Environment for Statistical Computing. Raetz-Brühlhart, H., 1997. Massenbewegungen im Gurnigelflysch und Einfluss der Klimäanderung. Ph.D. thesis. vdf Hochschulverlag AG, ETH Zürich, Zürich.
- Reardon, B.A., Pederson, G.T., Caruso, C.J., Fagre, D.B., 2008. Spatial reconstructions and comparisons of historic snow avalanche frequency and extent using tree rings in Glacier National Park, Montana, U.S.A. *Arctic, Antarctic, and Alpine Research* 40, 148–160.
- Reeder, J., 1979. The dating of landslides in anchorage, Alaska. A Case for Earthquake Triggered Movements, p. 501.
- Remaître, A., 2006. Morphologie et dynamique des laves torrentielles: Applications aux torrents des Terres Noires du bassin de Barcelonnette (Alpes du Sud). Ph.D. thesis. Université de Caen/Basse-Normandie.
- Rinntech, 2009. <http://www.rinntech.com/content/blogcategory/2/28/lang.english2009>.
- Ripley, B., 1996. *Pattern Recognition and Neural Networks*. Cambridge University Press, Cambridge; New York.
- Rolland, C., Florence-Schueller, J., 1998. Dendroclimatological synthesis on mountain pine (*Pinus uncinata* Mill. ex Mirb.) in the Pyrenees and the Alps. *Ecologie* 29, 417–421.
- Schuster, R., Wiczorek, G., 2002. Landslide triggers and types. In: Rybar, J., Stemberk, J., Wagner, P. (Eds.), *Landslides: Proceedings of the First European Conference on Landslides*, Prague, Czech Republic, pp. 59–78. June 24–26 2002.
- Shroder, J., 1978. Dendrogeomorphological analysis of mass movement on Table Cliffs Plateau, Utah. *Quaternary Research* 9, 168–185.
- Stefanini, M., 2004. Spatio-temporal analysis of a complex landslide in the Northern Apennines (Italy) by means of dendrochronology. *Geomorphology* 63, 191–202.
- Stien, D., 2001. Glissements de terrains et enjeux dans la vallée de l'Ubaye et le pays de Seyne. Rapport RTM.
- Stoffel, M., Perret, S., 2006. Reconstructing past rockfall activity with tree rings: some methodological considerations. *Dendrochronologia* 24, 1–15.
- Stoffel, M., Lièvre, I., Monbaron, M., Perret, S., 2005. Seasonal timing of rockfall activity on a forested slope at Täschgufer (Swiss Alps) – a dendrochronological approach. *Zeitschrift für Geomorphologie* 49, 89–106.
- Stoffel, M., Bollschweiler, M., Butler, D.R., Luckman, B.H., 2010. *Tree Rings and Natural Hazards: A State-of-The-Art*. Springer, Heidelberg, Berlin, New York. 505 pp.
- Therneau, T., Atkinson, E., 1997. *An Introduction to Recursive Partitioning Using the rpart Routine*. Technical Report Mayo Clinic, Rochester.
- Timell, T., 1986. *Compression Wood in Gymnosperms*. Springer-Verlag, Berlin, New York.
- Utasse, M., 2009. Cartographie morpho-dynamique et évolution historique de trois glissements actifs dans le bassin versant du Riou-Bourdoux (Alpes-de-Haute-Provence, Vallée de l'Ubaye). MSc Thesis. Université de Strasbourg, France.
- Van Den Eckhaut, M., Muys, B., Van Loy, K., Poesen, J., Beeckman, H., 2009. Evidence for repeated re-activation of old landslides under forest. *Earth Surface Processes and Landforms* 34, 352–365.